Superfluid Avalanches in Nuclepore: Constrained versus Free-Boundary Experiments and Simulations

A. H. Wootters* and R. B. Hallock†

Laboratory for Low Temperature Physics, Department of Physics, University of Massachusetts, Amherst, Massachusetts 01003, USA

(Received 7 January 2003; published 17 October 2003)

Superfluid ^{4}He exhibits hysteretic behavior in the percolated nanoporous material Nuclepore during the filling and draining of pores due to capillary condensation, and one observes avalanches during the pore draining. We observe that the size and frequency of the avalanches depend upon whether the fluid flow off the substrate during draining is impeded or unimpeded. We simulate the draining of superfluid ^{4}He from Nuclepore with and without a perturbation of the pore menisci and find results similar to the results seen in the experiments in the presence or the absence of flow inhibition.

DOI: 10.1103/PhysRevLett.91.165301 PACS numbers: 67.70.+n, 47.55.Mh, 67.40.Hf, 68.43.Mn

When superfluid ^{4}He is capillary condensed into the pores of Nuclepore [1](a nanoporous percolated polycarbonate membrane) and subsequently removed, one observes hysteresis in the adsorption/desorption curve and discrete avalanches during the draining [2]. In other words, a collection of pores comprising many pores distributed across the sample drains as a discrete event, behavior not seen in other fluid systems. We observe that when the superfluid film flow path from the sample during draining is impeded, the avalanches are larger in size, less frequent, and of longer duration than when the fluid has an unimpeded flow path off the sample. To gain some insight into the difference between these two cases and presuming that fluid draining from the pores will induce third sound [3], we successfully simulate the draining.

The Nuclepore polycarbonate membrane that we use is 10 μm thick, has a random spatial distribution of nearly cylindrical pores of nominal diameter 200 nm, and a pore density of $\psi_N = 3.5 \times 10^8$ pores/cm^2, with a random tilt angle θ of the axis of each pore from the normal to the surface, $0° \leq \theta \leq 34°$. The amount of ^{4}He in the Nuclepore is measured using a capacitance technique: 50 nm of Ag are evaporated onto each side of the Nuclepore membrane to form a capacitor. We take advantage of the dielectric nature of ^{4}He ($\kappa = 1.055$) to measure the change in the amount of fluid in the pores by measuring the change in capacitance as a function of changing chemical potential as ^{4}He is slowly and continuously added or removed from the sample cell at constant temperature T through a room temperature valve [4]. The capacitance is measured with a self-balancing bridge with resolution $\delta C/C \sim 5 \times 10^{-8}$. In the sample cell are Nuclepore substrates with one or more capacitors evaporated onto them and a borosilicate glass slide containing a driver and detector for measuring the speed of third sound waves, C_3. Third sound is a temperature and thickness wave on a superfluid ^{4}He film, and measurement of the speed of third sound induced on the flat glass substrate gives a convenient and stable measure of the *in situ* chemical potential μ_f in the experimental cell, $C_3^2 \sim (\mu_0 - \mu_f)$. Here μ_0 is the chemical potential of bulk liquid and μ_f is the chemical potential in equilibrium with the film thickness on the flat surface.

When the amount of fluid in the pores of a Nuclepore sample is measured as a function of chemical potential by measurements of the capacitance as a function of the third sound time of flight during adsorption and subsequent desorption, we observe a hysteresis curve that features a sharp drop in capacitance over a narrow range of chemical potential [circles, Fig. 1(a)]. When the capacitance is measured as a function of time, we observe avalanches in the draining [Fig. 1(b)]. In previous work, by looking at the time correlation between avalanches observed on two separate capacitors on a single piece of Nuclepore, we demonstrated that the avalanches involve a dilute collection of pores distributed across the entire substrate and that the avalanches are enabled by the presence of the superfluid film on the surface of the Nuclepore [2,4].

In our new experiments [5], capacitors (with area 0.95 cm × 0.95 cm) are evaporated onto two separate

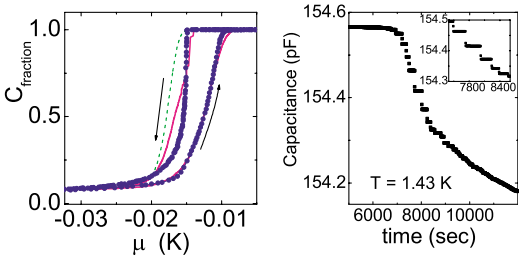

FIG. 1 (color online). (a) Adsorption/desorption isotherm for superfluid helium in Nuclepore. The solid symbols represent experimental data taken at $T = 1.48$ K for unimpeded flow (see text). The solid line shows our simulated results for interacting pores [see text near Fig. 3(d)]. The dashed line represents simulated draining if the pores drain independently according to surface diameters. (b) Capacitance as a function of time, illustrating avalanches in the draining of superfluid ^{4}He from Nuclepore.

Nuclepore samples that are contained in a copper sample chamber. One sample [denoted as limited flow (LF)] is connected to the surrounding sample can and film reservoir only by the wires attached to the capacitor. The flow velocity off the Nuclepore is limited by the critical velocity of the superfluid film. Thus, the flux of liquid helium from the Nuclepore by film flow is inhibited by the constraints imposed by the geometry in the LF case. In this situation, we observe that the largest avalanches have a duration of up to ~1.5 s [Fig. 2(a)]. The other sample [denoted as unimpeded flow (UF)] is well connected to the film reservoir; the edges of the sample are varnished to a piece of Nuclepore containing 400 nm diameter pores with a thin line of GE 7031 varnish. The ensemble is clamped to ~200 sheets of 400 nm Nuclepore. For this set of experiments, the duration of the avalanches is less than 0.11 s (the temporal resolution of our capacitance bridge), Fig. 2(b) [6].

When we determine the fractional avalanche size, $s = \Delta C/(C_{\text{full}} - C_{\text{empty}})$, as a function of the fraction of fluid remaining in the pores, $C_{\text{frac}} = (C - C_{\text{empty}})/(C_{\text{full}} - C_{\text{empty}})$ for each of the avalanches observed in a complete drain sequence for the samples, we observe quite different behavior for the two cases. Here ΔC is the size of an individual avalanche. For the UF case the size of the avalanches is less predictable as a function of fluid remaining in the substrate and they are smaller in size and more numerous than for the LF case [Figs. 3(a) and 3(b)]. For the LF case we see a relatively smooth and more monotonic relationship between avalanche size and filling fraction [Fig. 3(b)].

A plausible cause for the difference in avalanche behavior in the UF and LF cases is that, in the case of the LF substrate, the fluid cannot get off the substrate immediately after a collection of pores has drained and there is no unconstrained flow path off the substrate for a third sound wave [7]. We have conjectured that during the draining of a collection of pores, a third sound wave is induced on the surface of the Nuclepore as each pore drains and this can disturb the menisci of other pores enough to cause them to drain. We have demonstrated [2,4] that this is likely the case, and directly observed the stimulation of avalanches by the application of thermally induced third sound pulses [8]. A model calculation exploring the possible relevance of third sound to avalanche behavior has been performed by Guyer and McCall [3] and found to be qualitatively consistent with our observations. In the case of the LF substrate, one might imagine that third sound waves are at least partially reflected off the edges of the substrate, and the wave disturbances are therefore more effective at influencing menisci than would be the case if third sound passed over the substrate once and left the substrate without significant reflection. Our goal in our present effort to simulate avalanches in the draining of Nuclepore is to see if a model for such a mechanism of perturbative stimulation of avalanches by third sound waves of enhanced effectiveness is consistent with the data.

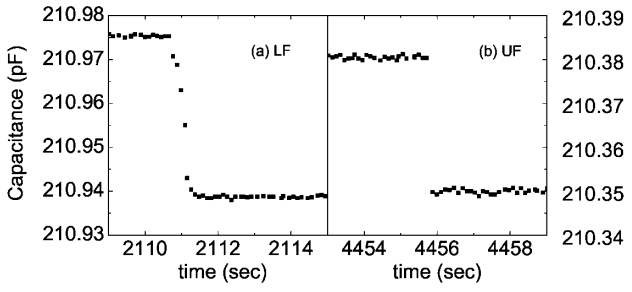

FIG. 2. (a) The solid symbols represent experimental data for the case of a single avalanche for the LF situation at $T = 1.567$ K. (b) An avalanche event for the UF situation at $T = 1.496$ K [6].

We carry out our simulation in two steps. We begin by neglecting the role of third sound. In order to simulate avalanches in Nuclepore, we modeled the connectivity of the pores as well as the filling and draining of the pores. Our model system consisted of a total of 5600 pores, randomly distributed on a horizontal plane, with a random azimuthal angle ϕ and a tilt angle from the normal to the plane, θ, $0° \leq \theta \leq 34°$, assigned to each pore. In reality, for nominal 200 nm Nuclepore the pores are somewhat barrel shaped; the average internal diameter by Brunauer, Emmett, and Teller and Langmuir fits has been estimated to be ~240 nm with a distribution of 20% [9]. The average diameter at the surface of the membrane is ~180 nm, with 200 nm as an upper limit. In view of this we assign an internal radius and surface radius to each pore. The pore diameter distribution is taken to be Gaussian and, per the manufacturer, the distribution in θ is taken to be linear.

To calculate the connectivity of the pores we use an average internal diameter of 240 nm with a normal

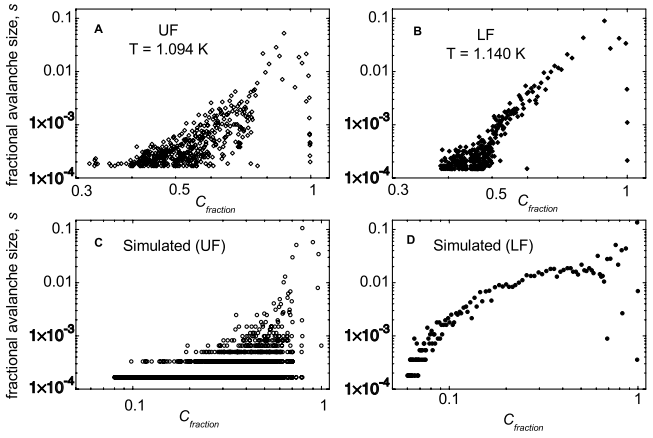

FIG. 3. Avalanche size distributions. Here, the fractional avalanche size, $s = \Delta C/(C_{\text{full}} - C_{\text{empty}})$ is shown as a function of the fraction of fluid remaining in the pores, $C_{\text{frac}} = (C - C_{\text{empty}})/(C_{\text{full}} - C_{\text{empty}})$ for (a) the UF experiment, (b) the LF experiment, (c) the UF simulation (see text), and (d) the LF simulation.

distribution of 20%. We define two pores to intersect if they at least touch (that is, the distance between the axes of the two pores is less than the sum of the pore radii). With such a definition, each pore is found to intersect an average of 6.5 other pores. Since intersection only matters here if fluid can drain through the intersection without creating an internal meniscus that will trap fluid, we consider two pores connected if the distance of closest approach between their two axes is less than half the sum of the two radii. Using this criterion, we determine that each pore is connected to an average of 3.2 other pores, well within the percolation limit.

The chemical potential at which an ideal cylindrical pore will capillary condense is determined by its internal diameter, but the chemical potential at which the ideal pore will drain is determined by the diameter of the pore where it intersects the membrane surface (or by the diameter of a larger pore with which it intersects in the interior of the sample). We assign filling (draining) chemical potentials as a function of internal (surface) diameters according to the approximate functions given by Cohen *et al.* [10]. The chemical potential inside a pore of radius R is given by $\mu_{\text{pore}} \approx -\alpha(\frac{a_\circ}{h_p})^3 - \frac{\sigma}{\rho(R-h_p)}$. The fluid in the pore will capillary condense when the film thickness inside the pore reaches a critical value. For a pore of diameter 240 nm, the critical film thickness inside the pore is $h_p \sim 45$ layers (one layer is taken to be 0.36 nm) , and the pore fills [11] at $\mu = -0.011$ K (with a flat surface film thickness of about 16.5 layers). We find that this critical value of h_p is not very sensitive to a 20% range of pore radii [12], so we approximate and use the same value of $h_p = 45$ layers for all radii. The accepted values of the constants [13,14] are $\alpha = 50$ K, $\rho = a_\circ^{-3}$, $a_\circ = 0.36$ nm, and $\sigma = 0.36$ erg/cm^2, leading to $\frac{\sigma}{\rho} = 1.22 \times 10^{-7}$ K cm. Using this general relationship between internal pore diameter and filling chemical potential, we assign a distribution of internal diameters so that our simulated adsorption curve fits the adsorption data portion of a typical hysteresis curve for nominal 200 nm Nuclepore [Fig. 1(a), adsorption, solid curve]. To accomplish this requires an average internal diameter of $240 \pm 43(18\%)$ nm.

The simulation of the draining of the pores is done by assigning two draining chemical potentials $\mu^i_{\beta,\text{inner}}$ and $\mu^i_{\beta,\text{top}}$ to each pore i. Each pore has an internal draining chemical potential $\mu^i_{\beta,inner}$, given by [10] $\mu^i_{\beta,\text{inner}} = -\frac{2\sigma}{\rho R_{i,\text{inner}}}$, where $R_{i,\text{inner}}$ is the internal radius of the pore determined by the adsorption curve. We assign reduced pore radius openings by the relationship $R_{i,\text{top}} = 0.15R_{i,\text{inner}} + x + f$. The parameter x is the average radius of the pore at the surface of the membrane (90 nm) and f is a rather arbitrary random additive factor, normally distributed about zero with standard deviation of 3 nm, included in an attempt to account for some of the geometric variations of Nuclepore introduced by the method of production. The corresponding draining chemical potential, $\mu^i_{\beta,\text{top}}$, is given by the same Kelvin equation, $\mu^i_{\beta,\text{top}} = -\frac{2\sigma}{\rho R_{i,\text{top}}}$. For the smaller internal radii ($R_{i,\text{inner}} < 106$ nm), the calculated $R_{i,\text{top}}$ is greater than $R_{i,\text{inner}}$, so for those values we set $R_{i,\text{top}} = R_{i,\text{inner}}$.

To determine the relationship between $R_{i,\text{top}}$ and $R_{i,\text{inner}}$, we set criteria in order to simulate the results of helium in Nuclepore. First, $R_{i,\text{top}} < 100$ nm for all pores. In order to simulate draining when $C_{\text{frac}} < 0.3$, where no avalanches are resolved, we further require that the draining for the later third of the draining be independent-pore draining [15]. Finally, we set $\frac{2\sigma}{\rho} = 1.75 \times 10^{-7}$ K cm in order to achieve draining onset at $\mu = -0.015$ K, the observed draining onset point [16].

We simulate a draining isotherm where internal connections are a factor in the draining. The largest connected-pore cluster contains $\sim$85% of the pores, thus a single avalanche is not the simple draining of clusters of connected pores. If it were, we would observe a largest avalanche size corresponding to 85% of the capillary condensed fluid instead of the 8%–12% we typically observe experimentally. We limit the draining by requiring that the internal draining chemical potential of a pore $\mu_{\beta,\text{inner}}$ be greater than or equal to the top draining chemical potential $\mu_{\beta,\text{top}}$ of the pore that is draining. In this way, we essentially demand that all of the fluid to drain during an avalanche drains through a single elected pore, and pores whose internal diameters are smaller than the surface diameter of the elected pore will not be part of the draining cluster.

We direct the draining as follows. Find the pore that has the largest μ_{top}. Look at all pores that are connected to this pore. Mark all pores j such that $\mu^j_{\beta,\text{inner}} > \mu_{\beta,\text{top}}$. That is, only let a connected pore drain if its internal draining chemical potential is greater than the chemical potential at which the original pore is draining. Next find the pores that are connected to the first generation of drained pores that have appropriate chemical potential values ($\mu^k_{\beta,\text{inner}} > \mu_{\beta,\text{top}}$), and so on, until all appropriate connected pores have been drained. A pore must be connected to a pore that has already drained in order to drain, even if it has sufficiently large $\mu_{\beta,\text{inner}}$. After all the pores of this cluster have been drained, the first avalanche is complete. To continue, we find the filled pore with the next largest $\mu_{\beta,\text{top}}$, identify the pores that are connected to it such that $\mu^j_{\beta,\text{inner}} > \mu_{\beta,\text{top}}$, drain them, and so on. As we empty pores, we keep track of how many pores drain in a single event (which corresponds to an avalanche) and how many pores remain filled as that collection of pores drains. When we restrict the draining this way, we find that the largest draining event is typically on the order of $\sim$10% of the total number of pores in the simulation, commensurate with what we observe in our experiments.

We apply this approach to a simulation sample of 5600 pores (corresponding to a sample of dimensions 40 μm $\times$ 40 μm $\times$ 10 μm), and "drain" the sample, keeping track of avalanche size as a function of the fraction of pores that

remain filled. Figure 1(a) (segmented solid line) shows the resulting draining portion of the hysteresis loop. For reference, if the pores were to drain independently, the resulting predicted hysteresis curve would be the smooth dashed line seen in Fig. 1(a). Figure 3(c) shows a plot of s vs C_{frac} for this simulation. Comparing this plot to that of a data plot for the UF substrate [Fig. 3(a)], we see the similarity of a largest avalanche size, and many avalanches of various sizes under an envelope that decreases with decreasing remaining fluid.

We next add a mechanism to simulate the perturbative effect (of third sound) to the model. Let pore i be the filled pore with the largest $\mu^i_{\beta,\text{top}}$ on the substrate. Drain that pore and the cluster associated with it, according to the rules noted previously. Before we consider the avalanche finished, however, we look at the filled pore j with the next largest $\mu^j_{\beta,\text{top}}$. If $|\mu^j_{\beta,\text{top}} - \mu^i_{\beta,\text{top}}| < \mu_{\text{thresh}}$, where μ_{thresh} is a threshold value that can be selected, we also drain that pore and the cluster associated with it. We consider that cluster to be part of the original avalanche. All pores with $\mu_{\beta,\text{top}}$ within the threshold limit of $\mu^i_{\beta,\text{top}}$ and their associated clusters are drained as part of a single avalanche, initiated by the draining of pore i. Thus we model the "overshoot" of avalanching, where pores that are nearly ready to drain are given the perturbation (caused in the experiments by the third sound thickness fluctuations) necessary to drain before they normally would. Figure 3(d) shows the resulting s vs C_{frac}. In this case, $\mu_{\text{thresh}} = 0.0002$ K. A choice of $\mu_{\text{thresh}} = 0.0$ K reproduces the behavior seen in Fig. 3(b). As μ_{thresh} increases (simulating an increasingly effective third sound perturbation) , the simulated avalanches become larger, less numerous, and less random in size as a function of C_{frac}.

A comparison of the plot of s vs C_{frac} for our model of avalanching with perturbations [Fig. 3(d)] and avalanching without perturbations [Fig. 3(c)] shows substantial similarities to a comparison to s vs C_{frac} plots for LF and UF substrates [Figs. 3(a) and 3(b)]. Figure 3(d) shows cleaner, more predictable s vs C_{frac} behavior than our UF model, where no perturbations are added, generally consistent with the data. In neither case does our model have time dependence and thus it does not allow prediction for the duration of avalanches.

Third sound is not required to cause avalanches, but its presence stimulates them, and, as we have shown in this work, enhancement of third sound changes the character of the avalanches. Explicitly, we have here observed that boundary constraints have a considerable influence on the dynamics of avalanche-dominated pore draining in the draining of superfluid ^{4}He from a nanoporous material. A reasonable model that includes fluctuation-stimulation of pore draining is able to reproduce many features that are observed in the experiments. This model helps to establish the relevance of third sound perturbations to the avalanche behavior seen in situations of constrained flow. We suspect that the distribution of pore draining events in any interacting physical system is influenced by the presence and lifetimes of perturbations to the system.

We thank Robert Guyer for helpful discussions and Michael Lilly for his earlier contributions to the general experimental apparatus. This work was supported by the National Science Foundation through DMR 98-19122 and DMR 01-38009.

*Present address: Department of Physics, Massachusetts College of Liberal Arts, North Adams, MA 01247, USA.
†Electronic address: hallock@physics.umass.edu

[1] Whatman International Ltd., Maidstone, England, and Tewksbury, MA.
[2] M. P. Lilly, P. A. Finley, and R. B. Hallock, Phys. Rev. Lett. **71**, 4186 (1993); M. P. Lilly, A. W. Wootters, and R. B. Hallock, Phys. Rev. Lett. **77**, 4222 (1996).
[3] R. A. Guyer and K. R. McCall, J. Low Temp. Phys. **111**, 841 (1998).
[4] M. P. Lilly and R. B. Hallock, Phys. Rev. B **63**, 174503 (2001); M. P. Lilly and R. B. Hallock, Phys. Rev. B **64**, 024516 (2001); M. P. Lilly, A. H. Wootters, and R. B. Hallock, Phys. Rev. B **65**, 104503 (2002).
[5] A. H. Wootters and R. B. Hallock, J. Low Temp. Phys. **126**, 211 (2002).
[6] The duration differences between the LF and the UF cases are robust to changes in temperature.
[7] The duration of the avalanche events on the LF substrate is consistent with the expected draining time for fluid flow from the substrate.
[8] M. P. Lilly, A. H. Wootters, and R. B. Hallock, Phys. Rev. B **65**, 104503 (2002), Table II, Fig. 13.
[9] D. S. Cannell and F. Rondelez, Macromolecules **13**, 1599 (1980); D. T. Smith, K. M. Godshalk, and R. B. Hallock, Phys. Rev. B **36**, 202 (1987); G. P. Crawford *et al.*, J. Chem. Phys. **96**, 7788 (1992).
[10] S. M. Cohen, R. A. Guyer, and J. Machta, Phys. Rev. B **33**, 4664 (1986).
[11] The curvature of the film surface in the pore has a large effect on the film thickness in the pore. When $h_p \sim 45$ layers, the flat surface thickness is $H \sim 16.5$ layers ($\mu \sim -0.011$ K); at draining onset, $H \sim 15$ layers ($\mu \sim -0.015$ K).
[12] When $\delta R = 20\%$, $\delta h_p = 2\%$.
[13] J. C. Noiray, D. Sornette, J. P. Romagnan, and J. D. LaHeurte, Phys. Rev. Lett. **53**, 2421 (1984).
[14] R. J. Donnelly and C. F. Barenghi, J. Phys. Chem. Ref. Data **27**, 1217 (1998).
[15] F. Preisach, Z. Phys. **94**, 277 (1935).
[16] The value $\frac{2\sigma}{\rho} = 1.75 \times 10^{-7}$ K cm differs from the accepted value of $\frac{2\sigma}{\rho} = 2.44 \times 10^{-7}$ K cm, but was required to provide an adequate fit to the draining onset at the observed $\mu = -0.015$ K. Given the fact that the pore openings of Nuclepore are far from uniform circles, we do not consider the difference between these two numbers significant.